Journal of Theoretical and Applied Information Technology
31st May 2022. Vol.100. No 10

ISSN: 1992-8645 www.jatit.org E-ISSN: 1817-3195

AN ENHANCED ACTIVE CONTOUR FOR IMAGE SEGMENTATION WITH STRONG NOISE

OMAR GOUASNOUANE[1,2], SOUMAYA BOUJENA[2], KARIMA KABLI[3]

[1]Laboratory of Mathematics, Computer Science and Applications (LMCSA),
University Hassan II of Casablanca, FST Mohammedia,
P.O Box 146, 20650, Morocco.
[2]Laboratory of Fundamental and Applied Mathematics (LMFA),
University Hassan II of Casablanca, Ain Chock Faculty of Science,
Km 8 Route d'El Jadida, B.P 5366 Maarif,
Casablanca, Morocco.
[3]Laboratory of Modelling, Analysis, Control and Statistics (MACS),
University Hassan II of Casablanca, Ain Chock Faculty of Science,
Km 8 Route d'El Jadida, B.P 5366 Maarif,
Casablanca, Morocco.
E-mail: [1,2]gouasnouane@gmail.com, [2]boujena@gmail.com, [3]smakarima@gmail.com.

ABSTRACT

Image segmentation is a useful and important technique in image processing, its purpose is to simplify and/or change the representation of an image into components that are more meaningful and easier to analyze. Nevertheless, even after the evolution of segmentation methods, they unfortunately lead to over-segmentation or to under-segmentation when applied to noisy images.

Among different techniques for the segmentation of pixels of interest from an image we focus on segmentation by active contour models. Those models have been widely successfully used, in recent years, for different applications. However, for noisy images it is necessary to perform a denoising preprocessing step for a satisfactory segmentation.

In this work we propose a segmentation model wich is a combination between a nonlinear diffusion model for image denoising and classical active contour models which use mean curvature motion techniques. For this we take, in the edge indicator function, the gradient of the image to be segmented which has been denoised by a nonlinear diffusion instead a Gaussian filter.

Finally, we will present various experimental results and in particular some examples for which the classical snakes methods based on the gradient are not applicable.

Keywords: *Image Segmentation, Level Set Methods, Nonlinear Diffusion, Nonlinear Diffusion, Active Contour Models.*

1. INTRODUCTION

Segmenting a digital image means finding by a numerical algorithm its homogeneous regions and their edges or boundaries. Of course, the homogeneous regions are supposed to correspond to meaningful parts of objects in the real world, and the edges to their apparent contours.

Image segmentation is frequently used in medical imaging for viewing organs and tissues for the purpose of diagnosis and treatment of many diseases. Some other main areas that use image segmentation extensively are computer vision and autonomous vehicles (see [16]).

There are various image segmentation procedures like active contours, split and merge segmentation, watershed segmentation, graph-based segmentation, mean shift segmentation and the normalized cut technic [19], [11]. Image segmentation, like many other tasks in image processing, has many difficulties [9]. One of the challenges of this procedure is the one developing approaches that can recognize complex objects, like those with sharp corners, holes, and mixed textures. Another difficulty of segmentation is the capacity to be able to recognize objects in an image even in presence of noise. The approach for segmentation adopted in this work is the famous active contours methods. In all the classical active contour models (see for instance [6], [7], [19] , [20]), an edge detector is used to stop the evolving curve on the boundaries of the desired object, usually this edge-function depending on the convolution of the image gradient with a Gaussian function. If the initial image is noised, then the isotropic smoothing Gaussian filter has to be strong, which will smooth the edges too and the evolving curve can't find the boundary. To overcome this, the idea is to combine a better performant image filtering to the segmentation processe. For this, a nonlinear filter model which preserves edges is applied and then the process of

active contour segmentation is engaged with a novel edge detector function which depends on the gradient of denoised image by this nonlinear restoration technic.

This paper is organized as follows. In the next section we review some steps of the nonlinear diffusion model employed. Section 3 contains a brief summary of image segmentation by geometric active contours implemented via level set methods. We end the paper validating our model by numerical results.

2. NONLINEAR DIFFUSION FOR IMAGE RESTORATION

Image restoration is historically one of the oldest concerns in image processing and is still a necessary preprocessing step for many applications. In recent decades, several mathematical nonlinear diffusion partial differential equations models for image restoration have been applied since the one of Perona and Malik was introduced, at first, in [17] in 1990. See for examples [1], [2], [3], [4], [7], [10], [13], [9], [19] and [12]. In this work we are interested to restore the noisy image using the following nonlinear model

$$\begin{cases} \dfrac{\partial v}{\partial t} - div\left(\mu_1\left(|\nabla v|\right)\nabla v\right) = 0, & in\, Q, \\ v(x,0) = v_0(x), & \forall x \in \Omega, \\ v(x,t) = 0, & \forall x \in \partial\Omega, \quad \forall t \in [0,T], \end{cases} \tag{1}$$

where v_0 is the grey level distribution of a given distorted image occupying a bounded domain Ω in $\mathbb{R}^2$ for which boundary is $\partial\Omega$. Q is defined by $Q = \Omega \times [0,T]$, for some given $T > 0$. And $|.|$ designs the $\mathbb{R}^2$ Euclidian norm.

The common characteristic of the nonlinear diffusion model is that over the region where the gradient of the image is small, the model acts like the heat equation on the other hand near the edges, where the gradient is large, the regularization is stopped and the edges are preserved. Typical example for an edge stopping function μ_1 which, in fact, has been used by the authors in [1]

$$\mu_1(s) = \frac{1}{1+\dfrac{s^2}{k^2}} + \theta \quad (k > 0). \tag{2}$$

θ is a positive constant and the parameter k is a measure for the steepness of an edge to be preserved: points with $s^2 > k$ are regarded as edges, where the diffusivity is small, whereas points with $s^2 < k$ are considered to belong to the interior of a region where the diffusivity is close to 1.

In [1] the authors establish that the model (1) is well posed in the Hadamard sense and admits a unique weak solution in Hilbert space $L^2\left(0,T,H^1(\Omega)\right)$ under suitable hypothesis on edge stopping function μ_1.

For the discretization of (1) we consider the Galerkin finite elements method. Given a triangulation T_h, we define the set $V_h \subset V$ of piecewise linear finite elements, i.e.

$$V_h = \{v \in C^0(\bar{\Omega}), v_{|T} \in \mathrm{P}_1 \quad \text{for all } \tau \in \mathrm{T}_h\},$$

the Galerkin finite element formulation of (1) is defined by:

Find $u_h \in V_h$ such that

$$\int_\Omega \frac{\partial u_h}{\partial t} v + \int_\Omega \mu_1\left(|\nabla u_h|\right)\nabla u_h \nabla v = 0, \tag{3}$$

that hold for all $v \in V$.

Then we apply, to each iteration in time, a semi-discretization: the nonlinear term of the equation is calculated from the results of the previous iteration while the linear terms are processed for the current iteration. We discretize the interval $[0;T]$ with uniform scaling interval Δt thus the discrete linear equation is

$$\int_\Omega \frac{u_h^n - u_h^{n-1}}{\Delta t} v + \int_\Omega \mu_1\left(\left|\nabla u_h^{n-1}\right|\right)\nabla u_h^n \nabla v = 0. \tag{4}$$

For this linear scheme we can proof the existence of a week solution in every discrete scale step by using theorem of Lax-milgram.

We denote by $\varphi_j \in V_h$ the standard Lagrangian bases functions, the function u_h^n is given by $u_h^n = \sum_{i=1}^{M} u_i^n \varphi_i$.

Let $v = \varphi_j(x)$, then equation (4) can be written

$$\sum_{i=1}^{M}\left\{\int_\Omega \varphi_i\varphi_j dx + \Delta t \int_\Omega \mu_1\left(\left|\nabla u_h^{n-1}\right|\right)\nabla\varphi_i\nabla\varphi_j\right\}u_i^n = \int_\Omega u_h^{n-1}\varphi_j dx. \tag{5}$$

Finally the discrete linear system is expressed as

$$\left(B + \Delta t A(\mu_1)\right)U^n = BU^{n-1}, \tag{6}$$

where

$$U^n = \left(u_1^n, u_2^n, \ldots, u_M^n\right)^t, \quad B_{ij} = \int_\Omega \varphi_i\varphi_j dx,$$

and $$A(\mu_1) = \int_\Omega \mu_1 \nabla\varphi_i \nabla\varphi_j dx. \tag{7}$$

3. SEGMENTATION BY GEOMETRIC ACTIVE CONTOUR

Existing active contour models can be classified according to their representation and implementation parametric active contour models [22]. Thus they can be considered as parametric active contour models as well as geometric active contour models. The parametric active contours are represented explicitly as parameterized curves in a Lagrangian framework, while the geometric active contours are represented implicitly as level sets of a two-dimensional function that evolves in an Eulerian framework. For a numerical point of view, we use the Eulerian formulation for a level set approach [14] is applied. This approach is based on the description of the curve as the zero crossing of a higher-dimensional function and allows major simplifications. There are many advantages to working with this Eulerian formulation. First, the contours represented by the level set function may break or merge naturally during the evolution, and the topological changes are thus automatically handled. Second, the level set function always remains a function on a fixed grid, which allows efficient numerical schemes. Finally, this above level set formulation can be extended and applied in any dimension.

3.1 Geometric active contour

The geometric active contour for image segmentation was introduced by Caselles et al. [4], it is based on the theory of curve evolution and the level set method. The contour C is represented by the zero level set of a level set function f. In the level set method the curve evolution of C is written in the following partial differential equation (PDE):

$$\frac{\partial \phi}{\partial t} = F\,|\nabla \phi|, \qquad (8)$$

where F is the speed function that controls the motion of the contour it depends on the image data and the level set function ϕ. This equation is completed by the initial condition ϕ_0 corresponding to the initial curve C_0.

The level set evolution in a early geometric active contour model is given by the following equation:

$$\frac{\partial \phi}{\partial t} = g(|\nabla I|)\, div\left(\frac{\nabla \phi}{|\nabla \phi|}\right) + \nabla g(|\nabla I|).\nabla \phi + \alpha g(|\nabla I|)|\nabla \phi|, \qquad (9)$$

where I is an image, α is a constant, and $g(|\nabla I|) = \frac{1}{1+|\nabla (G_\sigma * I)|^2}$ is an edge indicator function. This equation develops irregularities of ϕ during its evolution, which can cause numerical errors and destroys the stability of the evolution of the level set. To avoid this problem, we need to initialize the function ϕ as a signed distance function and periodically reshape it during the evolution by using this PDE equation:

$$\frac{\partial \phi}{\partial t} = sign(\phi)\,(1 - |\nabla \phi|), \qquad (10)$$

where ϕ is the level set function to be reinitialized, and $sign(\phi)$ is the sign function.

However, from a practical standpoint, the re-initialization can be quite complicated and expensive. To overcome this difficulty, Li et al. [8] recently introduced a new variational level set formulation in which the regularity of the level set function is maintained during the evolution and eliminates the need for re-initialization.

3.2 Distance regularized level set evolution

Li et al. propose in [8] a variational level set formulation that eliminates the need to re-initialisation and thus prevents its induced numerical errors. In contrast to complicated implementations of conventional level set formulations, a simpler and more efficient finite difference scheme can be used to implement this novel formulation.

Let I be an image, and g be the edge detector function satisfying

- g is regular monotonic decreasing.
- $g(0) = 1, \quad \lim_{s \to +\infty} g(s) = 0.$

A typical choice of g is $g(s) = \frac{1}{1+s^2}$, this function usually takes smaller values at object boundaries than at other locations.

The level set representation of the geodesic active contours proposed by Li et al. is written:

$$\frac{\partial \phi}{\partial t} = \gamma\, div\left(d_p(|\nabla \phi|)\nabla \phi\right) + \lambda \delta(\theta)\, div\left(g(|\nabla I|)\frac{\nabla \phi}{|\nabla \phi|}\right) + \alpha g(|\nabla I|)\delta(\phi), \qquad (11)$$

where $\mu > 0$, $\lambda > 0$ and α are constants, and

$$d_p(s) = \begin{cases} \frac{1}{2\pi s}\sin(2\pi s) & \text{if } s \le 1 \\ \frac{s-1}{s} & \text{if } s \ge 1 \end{cases}$$

The coefficient $g\left(|\nabla I|\right)$ permits one to stop the evolving curve when it arrives at the object boundaries. The first term penalizes the deviation of ϕ from a signed distance function and plays a key role in this model. The second and third term, correspond respectively to the gradient flows of the weighted length of the zero level set

Journal of Theoretical and Applied Information Technology
31st May 2022. Vol.100. No 10

ISSN: 1992-8645 www.jatit.org E-ISSN: 1817-3195

of ϕ and the weighted area of the region $\{(x,y)/\phi(x,y)<0\}$, respectively, would smoothly drive the motion of the zero level set toward the desired edges. Dirac function $\delta(.)$ is the derivative of one-dimensional Heaviside function.

Due to the penalizing term, the level set function driven by equation (11) is naturally and automatically kept as an approximate signed distance function during the evolution; therefore, the re-initialization procedure is completely eliminated. Also this level set evolution model has two main advantages over the traditional level set formulations. First, it can be implemented using a simple finite difference scheme instead of the complex upwind scheme as in traditional level set formulations, and a significantly larger time step can be used for solving equation (11) numerically. Second, the level set function ϕ can be efficiently initialized by a piecewise constant function as follows:

$$\phi_0(x,y)=\begin{cases}-\rho, & (x,y)\in R\\ 0, & (x,y)\in \partial R\\ +\rho, & (x,y)\in \Omega\setminus R\end{cases} \tag{12}$$

where R is an arbitrary open region in the image domain Ω, $\rho>0$ is a constant.

Then once ϕ is calculated on $\Omega\times\mathbb{R}_+$ we just need to extract the zero level set of ϕ to get the curve. Of course, we have to add the following conditions.

- A boundary condition: generally chooseen that the normal derivative vanishes on $\partial\Omega$ i.e. $\frac{\partial\Omega}{\partial n}=0$ on $\partial\Omega$.
- An initial condition at $t=0$.

Equation (11) is implemented with explicit difference scheme, the spatial derivatives are approximated by the central differences by using a fixed space steps $\Delta x=\Delta y=1$ and the temporal derivative is approximated by the forward difference. For the discretization of the term $|\nabla\varphi|div\left(\frac{\nabla\varphi}{|\nabla\varphi|}\right)$ there are several possible choices. (see for example [18]). To avoid the singularity at the point where the gradient of φ is null, $\nabla\varphi$ is approximated by:

$$|\nabla\varphi|\approx\sqrt{|\nabla\varphi|^2+\varepsilon} \text{ with } 0<\varepsilon\ll 1 \tag{13}$$

As in many level set methods the Dirac function δ is approximated by the following function δ_ν defined by :

$$\delta_\nu=\begin{cases}\frac{1}{2\nu}\left(1+\cos\left(\frac{\pi x}{\nu}\right)\right) & |x|\le\nu\\ 0 & |x|>\nu\end{cases} \tag{14}$$

By $\varphi_{i,j}^n$ and $I_{i,j}$ we denote approximation to $\varphi(x_i,y_j,t_n)$ and $I(x_i,y_j)$, respectively, where the partial derivatives are approximated by the following forward Euler differences:

$$D_x^+\varphi_{i,j}^n=\frac{\varphi_{i+1,j}^n-\varphi_{i,j}^n}{h},\quad D_y^+\varphi_{i,j}^n=\frac{\varphi_{i,j+1}^n-\varphi_{i,j}^n}{h} \tag{15}$$

Similary for $\frac{\partial I}{\partial x}$ and $\frac{\partial I}{\partial y}$.

The explicite discretization of (11) is given by:

$$\frac{\varphi_{i,j}^{n+1}-\varphi_{i,j}^n}{\Delta t}=\gamma G_{i,j}^n+\lambda\delta_\nu(\varphi_{i,j}^n)K_{i,j}^n+\alpha g(|\nabla I|_{i,j})\delta_\nu(\varphi_{i,j}^n) \tag{16}$$

where $|\nabla I|_{i,j}=\sqrt{(D_x^+I_{i,j})^2+(D_y^+I_{i,j})^2}$,

$$K_{i,j}^n=D_x^+\left(\frac{g(|\nabla I|_{i,j})D_x^+\varphi_{i,j}^n}{\sqrt{(D_x^+\varphi_{i,j}^n)^2+(D_y^+\varphi_{i,j}^n)^2+\varepsilon}}\right)+D_y^+\left(\frac{g(|\nabla I|_{i,j})D_y^+\varphi_{i,j}^n}{\sqrt{(D_x^+\varphi_{i,j}^n)^2+(D_y^+\varphi_{i,j}^n)^2+\varepsilon}}\right),$$

and

$$G_{i,j}^n=D_x^+\left(d_p(|\nabla\varphi_{i,j}^n|)D_x^+\varphi_{i,j}^n\right)+D_y^+\left(d_p(|\nabla\varphi_{i,j}^n|)D_y^+\varphi_{i,j}^n\right).$$

4. EXPERIMENTAL RESULTS

This section shows the simulation results of both model (1) and (11) for restoration and segmentation. To show the advantage of combining both models we use different types of images and same initial contour for each image. The model (11) is not sensitive to the choice of $\theta=10^{-6}$ and γ, which can be fixed for most of applications. The choice of the parameter $k=1$ is subject to the CFL condition. These parameters are fixed as $\lambda=5$, $\mu=0.04$, and time step $\Delta t=5$ in this paper. The parameter α needs to be turned for different images, if the initial contour is placed inside the object, the coefficient α should take negative value to expand the contour and if the initial contour is placed outside the object, the coefficient α should be positive, so that the zero level contour can shrink in the level set evolution. For the model (1) the parameters are fixed as $\theta=10^{-6}$ and $k=1$.

For the examples in figures 1-6, we show the image and the evolving contour. In all cases, we start with a very

Journal of Theoretical and Applied Information Technology
31st May 2022. Vol.100. No 10

ISSN: 1992-8645 www.jatit.org E-ISSN: 1817-3195

noisy image and a single initial closed curve. We show how our model (see cell d) can restore image and detect contours compared with classical active contours based on the gradient or Gaussian smoothing gradient for edge function.

5. Conclusion

In this paper we propose a modified active contour model for image segmentation. It's a combination between a classical active contour models using mean curvature motion techniques, and a nonlinear diffusion model for denoising and segmentation. In the classical active contour models the edge indicator function is based on a Gaussian filter, to stop the evolving curve on the desired boundary while, in the proposed model we replace it by a function which depends on the gradient of the restored image by a nonlinear diffusion filter. In this way the locations of boundaries are very well detected as shown in the different numerical simulations presented that validate our model.

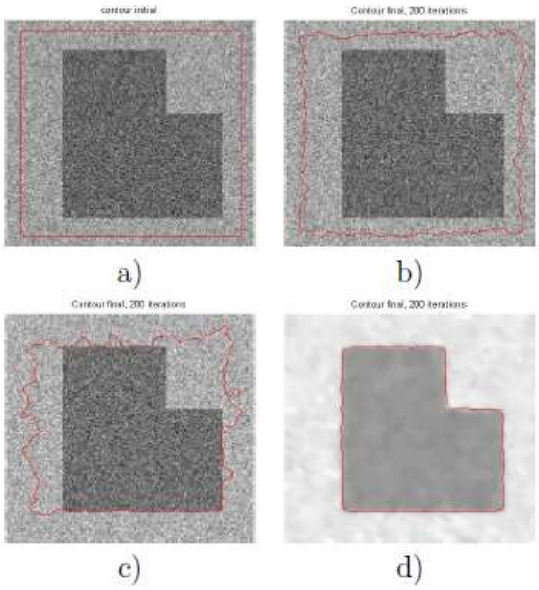

Figure 1: Results of segmentation using model (11) after 200 iterations using different edge indicator functions with $\alpha = 2$, $\lambda = 5$, $\gamma = 0.04$, *and time step* $\Delta t = 5$. *a) Noisy image and initial contour. b) Detection result with edge indicator function* $g\left(|\nabla I|\right) = \frac{1}{1+|\nabla I|^2}$. *c) Detection result in restored image by Gaussian filter with edge indicator function* $g\left(|\nabla I|\right) = \frac{1}{1+|\nabla G_\sigma * I|^2}$. *d) Detection result after restoration using edge indicator function* $g\left(|\nabla \hat{I}|\right) = \frac{1}{1+|\nabla \hat{I}|^2}$ *with* $\hat{I}$ *is restored image by (1).*

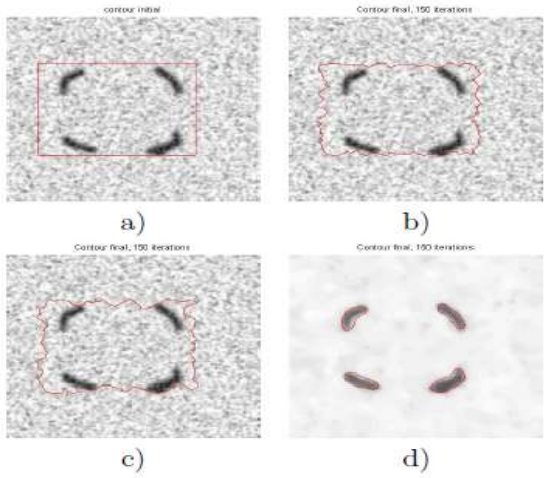

Figure 2: Results of segmentation using model (11) after 150 iterations using different edge indicator functions with $\alpha = 2$, $\lambda = 5$, $\gamma = 0.04$, *and time step* $\Delta t = 5$. *a) Noisy image and initial contour. b) Final result after 150 iterations using edge indicator function* $g\left(|\nabla I|\right) = \frac{1}{1+|\nabla I|^2}$. *c) Final result after150 iterations using edge indicator function* $g\left(|\nabla I|\right) = \frac{1}{1+|\nabla G_\sigma * I|^2}$. *d) Final result after150 iterations using edge indicator function* $g\left(|\nabla \hat{I}|\right) = \frac{1}{1+|\nabla \hat{I}|^2}$ *with* $\hat{I}$ *is restored image by (1).*

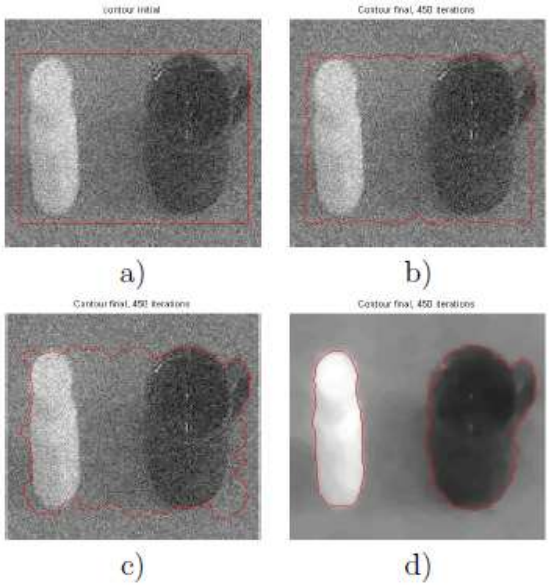

Figure 3: Results of segmentation using model (11) after 450 iterations using different edge indicator functions with $\alpha = 2$, $\lambda = 5$, $\gamma = 0.04$, *and time step* $\Delta t = 5$. *a) Noisy image and initial contour. b) Final result after 450 iterations using edge indicator function . c) Final result after 450 iterations using edge indicator function*

$g(|\nabla I|)=\frac{1}{1+|\nabla G_\sigma * I|^2}$ *. d) Final result after 450 iterations using edge indicator function* $g\left(\left|\nabla \hat{I}\right|\right)=\frac{1}{1+\left|\nabla \hat{I}\right|^2}$ *with* $\hat{I}$ *is restored image by (1).*

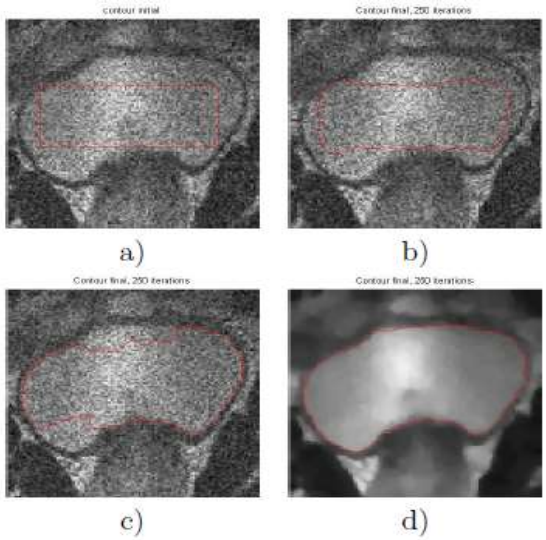

Figure 4: Results of segmentation using model (11) after 250 iterations using different edge indicator functions with $\alpha=-2.7,\ \lambda=5,\ \gamma=0.04$*, and time step* $\Delta t=5$*. a) Noisy image (Gaussian and speckle) and initial contour. b) Final result after 250 iterations using edge indicator function* $g(|\nabla I|)=\frac{1}{1+|\nabla I|^2}$ *. c) Final result after 250 iterations using edge indicator function* $g(|\nabla I|)=\frac{1}{1+|\nabla G_\sigma * I|^2}$ *. d) Final result after 250 iterations using edge indicator function* $g\left(\left|\nabla \hat{I}\right|\right)=\frac{1}{1+\left|\nabla \hat{I}\right|^2}$ *with* $\hat{I}$ *is restored image by (1).*

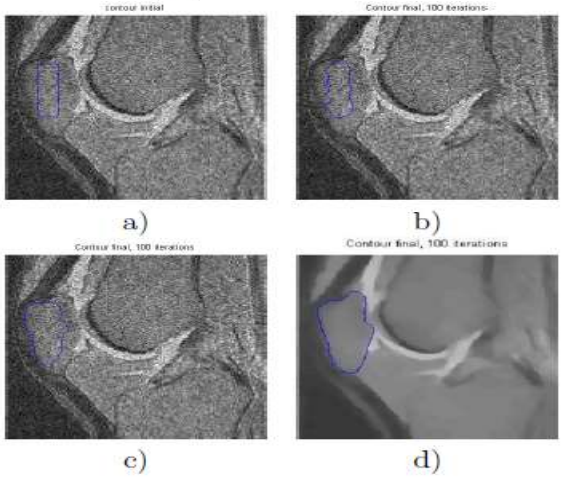

Figure 5: Results of segmentation using model (11) after 100 iterations using different edge indicator functions with $\alpha=-2.8,\ \lambda=5,\ \gamma=0.04$*, and time step* $\Delta t=5$*. a) Noisy image (Gaussian and speckle) and initial contour. b) Final result after 100 iterations using edge indicator function* $g\left(\left|\nabla I\right|\right)=\frac{1}{1+\left|\nabla I\right|^2}$ *. c) Final result after 100 iterations using edge indicator function* $g(|\nabla I|)=\frac{1}{1+|\nabla G_\sigma * I|^2}$ *. d) Final result after 100 iterations using edge indicator function* $g\left(\left|\nabla \hat{I}\right|\right)=\frac{1}{1+\left|\nabla \hat{I}\right|^2}$ *with* $\hat{I}$ *is restored image by (1).*

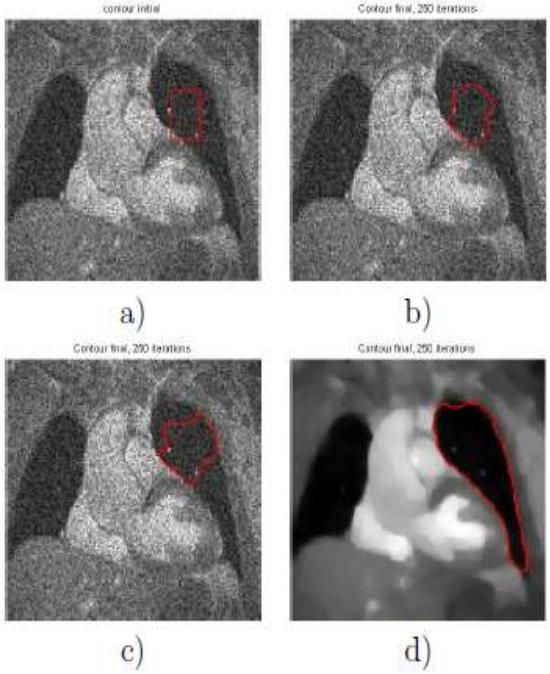

Figure 6: Results of segmentation using model (11) after 250 iterations using different edge indicator functions with $\alpha=-2,\ \lambda=5,\ \gamma=0.04$*, and time step* $\Delta t=5$*. a) Noisy image (Gaussian+speckle) and initial contour. b) Final result after 250 iterations using edge indicator function* $g\left(\left|\nabla I\right|\right)=\frac{1}{1+\left|\nabla I\right|^2}$ *. c) Final result after 250 iterations using edge indicator function* $g(|\nabla I|)=\frac{1}{1+|\nabla G_\sigma * I|^2}$ *. d) Final result after 250 iterations using edge indicator function* $g\left(\left|\nabla \hat{I}\right|\right)=\frac{1}{1+\left|\nabla \hat{I}\right|^2}$ *with* $\hat{I}$ *is restored image by (1).*

REFERENCES:

[1] R. Aboulaich, S. Boujena, and E. EL Guarmah, "A Nonlinear Parabolic Model in Processing of Medical Image", *Math. Model. Nat. Phenom.*, Vol. 3, No. 6, 2008, pp. 131-145. doi:10.1051/mmnp:2008084.

[2] R. Aboulaich, S. Boujena, and E. EL Guarmah, "Sur un modèle non-linéaire pour le débruitage de l'image", *C.R. Acad. Sci. Paris. Ser. I*, Vol. 345, No. 8, 2007, pp. 425-429. doi : 10.1016/j.crma.2007.09.009.

[3] S. Boujena , E. El Guarmah, O. Gouasnouane, J. Pousin, "On a derived non linear model in image restoration", *Proceedings of 2013 International Conference on Industrial Engineering and Systems Management, IEEE – IESM, 2013*, pp. 1-3.
https://ieeexplore.ieee.org/document/6761435.

[4] V. Caselles, F. Catte, T. Coll, and F. Dibos, "A geometric model for active contours in image processing", *Numer. Math.*, Vol. 66, No. 1, 1993, pp. 1-31.
https://doi.org/10.1007/BF01385685.

[5] V. Caselles, R. Kimmel and G. Sapiro, "On geodesic active contours", *Journal of Computer Vision*, Vol. 22, No. 1, 1997, pp. 61-79.

[6] F. Catt, P. L. Lions, J. M. Morel, and T. Coll, "Image selective smoothing and edge detection by a nonlinear Diffusion", *SIAM Journal on Numerical Analysis*, Vol. 29, No. 1, 1992, pp. 182-193.
doi - 10.1137/0729052.

[7] A. Chambole, P. L. Lions "Image recovery via total variation minimization and related problems", *Numer. Math*., Vol. 74, No. 2, 1997, pp. 147-188.
https://doi.org/10.1007/s002110050258.

[8] L. Chunming, X. Chenyang, "Distance Regularized Level Set Evolution and its Application to Image Segmentation", *IEEE transactions on image processing*, Vol. 19, No. 12, 2010, pp. 3243-3254.
doi: 10.1109/TIP.2010.2069690.

[9] I. Despotović, B. Goossens, W. Philips, "MRI Segmentation of the Human Brain: Challenges, Methods, and Applications", *Computational and Mathematical Methods in Medicine*, Vol. 2015, No. 6, 2015, pp. 1-23.
https://doi.org/10.1155/2015/450341.

[10] P. Guidotti, "A family of nonlinear diffusions connecting Perona-Malik to standard diffusion", *Discrete and Continuous Dynamical Systems - Series S*, Vol. 5, No. 3, 2012, pp. 581-590. doi: 10.3934/dcdss.2012.5.581.

[11] K. Haris, S.N. Efstratiadis, N. Maglaveras, A.K. Katsaggelos, "Hybrid image segmentation using watersheds and fast region merging", *IEEE Trans Image Process.*, Vol. 7, No. 12, 1998, pp. 1684-99.
doi: 10.1109/83.730380. PMID: 18276235.

[12] M. Kass, A. Witkin, D. Terzopoulos, "Snakes: Active contour models", *International Journal of Computer Vision,* Vol. 1, No. 1, 1988, pp. 321-331.

[13] S. Levins,Y. Chen, and J. Stanich, "Image restoration via nonstandard diffusion", *Technical-Report 04-01, Dept. of Mathematics and Computer Science, Duquesne University*, 2004.
doi=10.1.1.62.4573.

[14] C. Li, R. Huang, Z. Ding, C. Gatenby, D.N. Metaxas, J.C. Gore, "A Variational Level Set Approach to Segmentation and Bias Correction of Images with Intensity Inhomogeneity", *Medical image computing and computer-assisted intervention : MICCAI International Conference on Medical Image Computing and Computer-Assisted Intervention 11 Pt 2*, 2008, pp. 1083-91.

[15] R. Malladi, J.A. Sethian and B.C. Vemuri, "A Topology Independent Shape Modeling Scheme", *Proc. SPIE Conf. on Geometric Methods in Computer Vision II, San Diego*, Vol. 2031, No. 1, 1993, pp. 246-258.

[16] J.-M. Morel, S. Solimini, "Variational methods in image segmentation: With seven image processing experiments", *Boston: Birkhäuser*, 1995, http://books.google.com
/books?id=6-ZRAAAAMAAJ.

[17] P. Perona, J. Malik, "Scale-space and edge detection using anisotropic diffusion", *IEEE Transaction on Pattern Analysis and Machine Intelligence*, Vol. 12, No. 7, 1990, pp. 429-439.
doi: 10.1109/34.56205.

[18] L. Rudin, S. Osher, and E. Fatemi, "Nonlinear total variation based noise removal algorithms", *Physica D*, Vol. 60, No. 1-4, 1992, pp. 259-268.
https://doi.org/10.1016/0167-2789(92)90242-F

[19] R. Szeliski, "Segmentation", In: *Computer Vision*. Texts in Computer Science. Springer, London, 2011. https://doi.org/10.1007/978-1-84882-935-0_5.

[20] J. Weickert, "Anisotropic Diffusion in Image Processing", PhD thesis, University of Kaiserslautern, Germany, Laboratory of Technomathematics. January, 1996.
https://www.mia.uni-saarland.de /weickert/Pa-pers/book.pdf.

[21] J. Weickert, M. Bart, H. Romeny ter, and A. Viergever Max, "Efficient and reliable Schemes for nonlinear Diffusion Filtering", *IEEE Trans., Image Processing*, Vol. 7, No. 3, 1998, pp. 398-410.
doi: 10.1109/83.661190.

[22] C. Xu, A. Yezzi, J.L. Prince, "On the relationship between parametric and geometric active contours", *Conference Record of the Thirty-Fourth Asilomar Conference on Signals, Systems and Computers (Cat.* No.00CH37154) , Vol. 1, No. 1, 2000, pp. 483-489. doi: 10.1109/ACSSC.2000.911003.